

Investigation of the atomic structure of Si(100) surfaces covered by submonolayer Bi films

R. Z. Bakhtizin

Physics Faculty, Bashkir State University, 450074 Ufa, Russia

C. Park

Physics Faculty, Jeonbuk National University, 560-756 Jeonju, South Korea

T. Hashizume and T. Sakurai

Institute for Materials Research, Tohoku University, 980 Sendai, Japan

(Submitted 11 March 1995)

Zh. Éksp. Teor. Fiz. **108**, 977–989 (September 1995)

Scanning tunneling microscopy (STM) and low-energy electron diffraction have been used to investigate the $(2 \times n)$ phases formed on a Si(100)- (2×1) surface when bismuth is adsorbed. A series of ordered $(2 \times n)$ superlattices with a periodicity n ranging from 5 to 12, which depends on the Bi coverage θ and the annealing temperature, have been observed. The STM images convincingly show that the $(2 \times n)$ structures are the result of the formation of periodic rows of missing bismuth dimers; however, the ordering in the arrangement of the missing rows in phases with n smaller than 5 is violated because of the competitive generation of linear defects and defects of rectangular shape. The formation of successive $(2 \times n)$ phases as a function of the coverage permits postulating the appearance of long-range elastic repulsion between the missing rows of bismuth dimers. A structural model of the Bi/Si(100) system, which accounts for all the types of surface defects observed, has been proposed. © 1995 American Institute of Physics.

1. INTRODUCTION

The investigation of the structure of adsorbed layers and the phase transitions in them is one of the most important areas in the physics of surfaces.¹ There is special interest in the analysis of the crystal and electronic structure of atomically clean silicon surfaces covered with films of various metals both from the standpoint of studying the fundamental properties of the metal–semiconductor boundary (especially in the early stages of the formation of such a junction) and from the standpoint of numerous technological applications in semiconductor microelectronics.² The reconstruction of the surface observed here generally lowers its free energy due to a decrease in the number of dangling bonds owing to the formation of new bonds either between the surface atoms themselves (rehybridization of the interatomic bonds) or between adsorbate atoms and surface atoms. Such redistribution of the dangling bonds, which makes it possible to bind all the free valences on the surface, can be a source of considerable structural distortions. The balance between the energy released as a result of the decrease in the number of dangling bonds and the energy of the elastic strains appearing in the adsorbed layer is specifically responsible for the appearance of various superstructures on the surface, particularly the ordered phases consisting of one-dimensional linear structures that are often observed in various physically adsorbed and chemisorbed systems.

For this reason there should be considerable interest in the study of the adsorption of bismuth on Si(111)- (7×7) and, especially, Si(100)- (2×1) surfaces, which differ significantly with respect to both their geometric structure and

the number of dangling bonds. Since the atomic radius of Bi (1.55 Å) significantly exceeds the atomic radius of Si (1.18 Å), the appearance of considerable structural distortions and attendant elastic strains, as well as the familiar structural transition between commensurate and incommensurate solid phases on a surface, can be expected in adsorbed bismuth films. As we know, a phase transition between commensurate $(1 \times n)$ phases with the same orientation is usually produced in systems by means of continuous compression of the adsorbed layer in one direction (along the “ n ” direction), and theories concerning superstructures of the domain-wall type are often utilized to interpret the additional reflections observed in this case on the corresponding low-energy electron diffraction (LEED) patterns.^{1,3} The investigation of the surface stresses appearing in this process has become interesting in itself in recent years owing to their conspicuous manifestations in surface reconstruction, melting, and segregation processes, as well as in interfacial mixing.^{3–7} For example, Butz *et al.*, observed additional surface deformation caused by the segregation of Ge in doped SiGe layers on a Si(100) surface.⁵ Tromp *et al.* recently reported the adsorption of As on a Si(100) surface, which is associated with the replacement of a portion of the surface atoms, and theorized that the surface tension can serve as the driving force for interfacial mixing.⁷

Another argument in favor of the performance of such investigations is the fact that a Si surface can be passivated completely, all the dangling bonds can be eliminated, and the bulk structure can be reproduced when group-III and group-V elements are adsorbed, as we demonstrated for the Bi/Si(111) system in Ref. 8. In the case of a Si(100) surface

with a highly anisotropic atomic relief, each surface atom maintaining the bulk geometry is bonded to two other atoms and has two dangling bonds. Then, the adsorption, for example, of group-V elements can result in saturation of all the dangling bonds by means of the formation of dimers of adsorbate atoms, each of which is bonded to two silicon atoms.

The adsorption of such group-V semimetals as As (Refs. 9 and 10) and Sb (Refs. 11 and 12) is known to result in destruction of the Si(100)-(2×1) superstructure and passivation of the surface. For example, the investigation of the Sb/Si(100) system by photoelectron spectroscopy in Ref. 13 revealed a distribution of the density of occupied bulk electronic states, thereby confirming the passivation of the Si(100)-(2×1) surface caused by the adsorption of Sb. It was also reported in Refs. 11 and 12 that Sb and As atoms form chains of dimers perpendicular to the chains of silicon dimers. We note that Bi, which is also a group-V element, forms a (2×*n*) structure on a Si(100) surface. For example, Hanada and Kawai¹³ postulated on the basis of an analysis of the results of their own photoemission experiments that the dangling bonds on a Si(100)-(2×1) surface are eliminated when Bi is adsorbed. In a subsequent investigation of the same system using reflection high-energy electron diffraction (RHEED), they showed that bismuth forms a (2×*n*) superlattice, which undergoes a continuous transformation from *n*=5 to *n*=13 during the successive adsorption of Bi, and they explained the latter by proposing a reconstruction mechanism involving the formation of missing rows of dimers.¹⁴ However, after studying the Bi/Si(100) system by LEED together with an analysis of the dependence of the intensity of the diffraction reflections on the electron energy, Fan *et al.*, reported the observation of a (1×1) structure at monolayer coverage and arrived at the conclusion that although no long-range order appears in the structure of the adsorbed bismuth atoms, they participate in the stabilization of the (1×1) structure on a Si(100) surface.¹⁵

Unlike the surfaces of metals, for both clean and adsorbate-covered surfaces of semiconductors, particularly Si(100), there are only a few known examples (besides those cited above) of the formation of (2×*n*) structures and phase transitions between them. In the case of a clean Si(100)-(2×1) surface, (2×*n*) structures, where *n* varied as a function of the annealing temperature from 6 to 9, were observed using LEED and interpreted on the basis of a mechanism for the ordering of rows of missing-dimer defects.^{16,17} Ordered periodic linear defects in the form of individual missing rows repeating after every four rows of dimers were also observed on Si(100) surfaces subjected to ion bombardment and annealing in Ref. 18. An STM investigation of the ordering of missing rows of dimers in Si(100)-(2×8) structures stabilized by a Ni impurity was reported in Ref. 19, and the observation of (2×*n*) structures with *n*=8 formed by Ge films and SiGe layers on a Si(100) surface were observed in Ref. 5.

In this communication we present the results of a detailed (on the atomic level) STM investigation of (2×*n*)-Bi structures on a Si(100)-(2×1) surface at different coverages and annealing temperatures, which revealed the presence of a series of ordered (2×*n*) superlattices and

showed that the formation of these structures is the result of the ordering of missing-row defects and the accompanying processes that occur to remove stresses in the strained Bi layer. Interest in the Bi/Si(100) system arises, in addition, because bismuth is a semimetal with a small electron effective mass in the direction of film growth, which is widely employed in micro- and nanoelectronics, since it forms ordered layers on substrates and promotes heteroepitaxial growth, for example, of the Si/Ge system, and which displays a size effect when it is adsorbed.²

2. METHOD

The experiments were performed in a state-of-the-art ultrahigh-vacuum STM system with a residual pressure in the working chamber equal to 5×10^{-11} Torr, which was equipped with a field-ion microscope (FIM) for improving and monitoring the quality of the scanning tips, as well as an additional chamber for sample preparation with a built-in ULA-020 unit, which consists of a low-energy electron diffraction camera and an Auger spectrometer, for preliminary structural analysis of the surface and evaluation of the Bi coverage. The scanning tips were prepared from a single-crystal W wire with the $\langle 111 \rangle$ orientation. Tungsten was chosen because the density of states of the conduction electrons near its Fermi surface contains an isotropic *s/p* component, which makes the main contribution to the tunneling current in the STM geometry, while the orientation selected ensures long-term stability of the tip shape. The final tip shape, which contains only one to three atoms at its apex (this is of fundamental importance for obtaining true atomic resolution in STM²⁰), was obtained by field vaporization at room temperature with continual monitoring using the FIM. The details of the STM experiment were described in Ref. 21. Samples of rectangular shape measuring 320×5×0.5 mm were cut from boron-doped silicon single crystals with a resistivity of 3.0 Ω·cm and the $\langle 100 \rangle$ orientation. The surfaces of the samples were cleaned by a series of high-temperature annealings at up to 1230 °C. The Bi layers were deposited by thermally sputtering a chip of metallic bismuth of purity 5N, which was placed in a tantalum Knudsen effusion cell.

3. RESULTS AND DISCUSSION

A series of (2×*n*) surface structures with different Bi coverages were obtained by subjecting several bismuth layers preliminarily deposited on the surface of a sample at room temperature to annealing at a gradually increasing temperature. Single-crystal Bi films are known to grow on Si(100) according to the Stranski–Krastanov mechanism. The desorption of three-dimensional bismuth islands begins at *T*=200 °C, while the two-dimensional (2×*n*)-Bi layers are maintained up to *T*=500 °C (Refs. 14 and 22). Thus, the value of the thickness of the original Bi layer deposited at room temperature did not significantly affect the results presented below for coverages exceeding one monolayer. As Bi was deposited on a clean Si(100)-(2×1) surface at room temperature (Fig. 1a), the intensity of all the reflections on the diffraction pattern gradually decreased, and (ultimately)

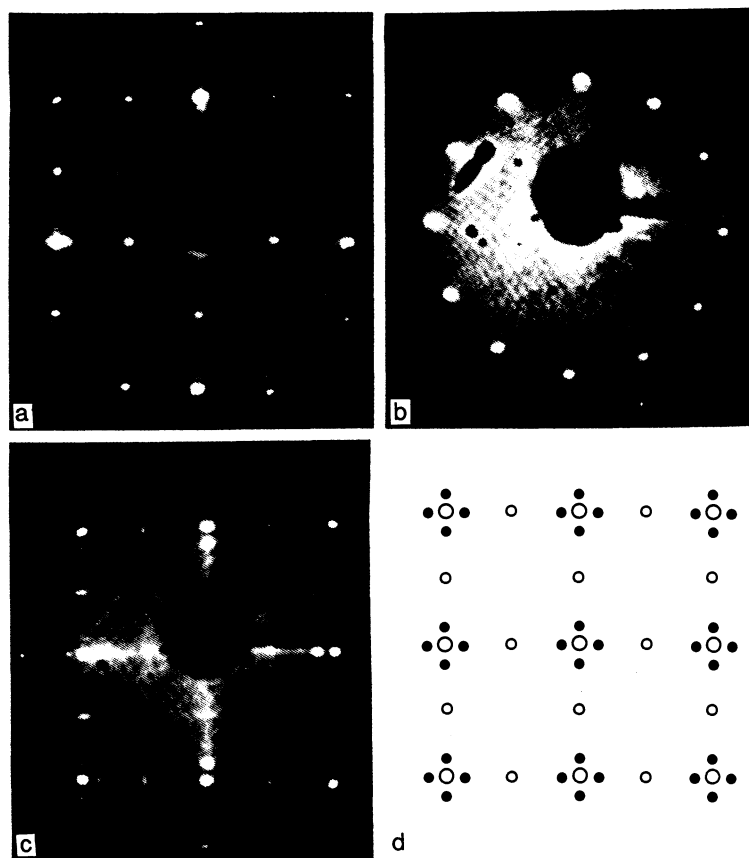


FIG. 1. LEED patterns of bismuth layers deposited on an atomically clean Si(100) surface: a) original clean Si(100)-(2×1) surface, $E=34$ eV; b) after the deposition of a thick layer of Bi, $E=30$ eV; c) after annealing of the Bi layer for 5 min at 378 °C, $E=34$ eV (the n th-order reflections are located at a distance equal to $d=\frac{1}{n}a$, where the lattice constant is $a=3.84$ Å); d) corresponding geometric diagram of the positions of the principal and additional reflections. /.

the reflections of half-integer order practically disappeared, being replaced by a disordered (1×1) structure. The further deposition of Bi resulted in the appearance of an annular structure with 12 reflections evenly spaced around it (Fig. 1b), indicating the epitaxial growth of Bi layers, in which the Bi(0001) plane grows parallel to the Si(100) surface predominantly for two azimuthal orientations, in good agreement with the results in Ref. 13. During annealing at $T>200$ °C, appreciable thermal desorption of three-dimensional Bi crystallites began, and the hexagonal structure was replaced by the pattern for a (2×1) structure with additional n th-order reflections around the reflections of integer and half-integer order, as is shown in Fig. 1c and is schematically represented in Fig. 1d. As the annealing temperature was raised, the distance between the principal and additional reflections continually increased, allowing us to regard the pattern obtained as a (2× n) superlattice.

A series of photographs of the LEED patterns for different annealing temperatures was prepared to obtain the quantitative dependence of $n(T)$. As is seen from Fig. 2, the variable n takes on both integer and fractional values and decreases from 12 to 5 as the annealing temperature rises. This result is in good agreement with the data from the RHEED experiments in Ref. 14, which were, however, obtained at higher temperatures, and shows that the transition between (2× n) phases is irreversible and is most probably caused by a decrease in the two-dimensional Bi coverage during successive annealing procedures. It is important to stress here that values of n smaller than 5 were not observed in our experiments, so that the (2×5) phase apparently re-

mains stable up to the complete desorption of Bi. At $T\geq 520$ °C all the Bi atoms are desorbed, and the clean (2×1) surface is restored; however, it should be noted that eighth-order reflections appeared again immediately before the return to the clean (2×1) structure.

Figure 3a presents the STM image of a portion of a Si(100) surface covered by bismuth, which displays the characteristic fine features of the structures formed at the atomic level. This overlayer was obtained after annealing a preliminarily deposited Bi layer at $T=378$ °C for 5 min and corresponds to the LEED pattern in Fig. 1c, i.e., to a (2× n) structure with $n=6.8$ (Fig. 2). This image clearly shows collections (stripes) of rows of atoms with (2×1) periodicity and periodically (at $n=7$) missing rows of Bi. Each stripe contains six (i.e., $n-1$) atomic protrusions in the direction perpendicular to the missing rows, which, in turn, are regularly arranged at a distance of $7a$ from one another.

It can be confidently assumed from the form of the image under discussion that missing rows separated by n rows of atoms are responsible for the multiple-scattering reflections on the electron diffraction patterns when additional diffraction peaks appear in the unit cell of the reciprocal lattice at $1/n$. Without the information obtained from the STM images, the interpretation of the LEED patterns could easily lead to erroneous conclusions. Moreover, the periodicity of the missing rows was scarcely violated over the entire sample surface investigated and is in good agreement with the (2×7) superlattice observed on the LEED patterns (Fig. 1c). We note, nevertheless, that the STM image of the surface analyzed (Fig. 3a) exhibits all the types of defects which

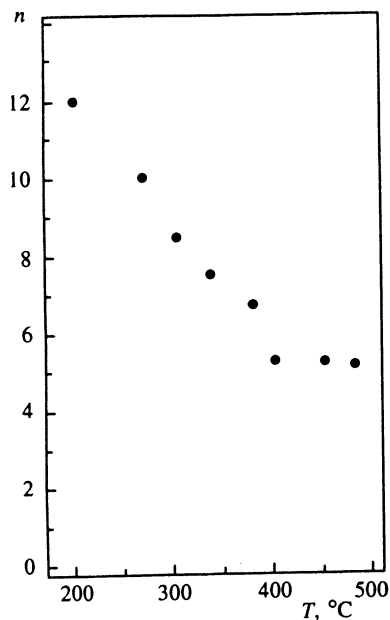


FIG. 2. Temperature dependence of the order n for $(2 \times n)$ structures on a Si(100)-(2 \times 1) surface.

are characteristic of this case: single linear defects perpendicular to the regular missing rows, vacancies of rectangular shape, and a certain number of three-dimensional Bi crystallites, which are predominantly square.

Figure 3b presents the STM image of a portion of the same surface, but with a far greater area, on which long-range order can be observed in the arrangement of the missing-row defects, and long stripes of $(2 \times n)$ structures, separated by missing Bi rows with almost ideal periodicity, can be seen, which totally cover the terraces on the silicon surface.

The structure under discussion is very reminiscent of the arrangement of the rows of dimers on a clean Si(100)-(2 \times 1) surface, with the exception of the existence of ordered missing rows. At the same time, although this structure also contains regions with some local disorder, it is perfectly clear that it is a mixture of different domains of $(2 \times n)$

structures. At high Bi coverages, which were achieved during the annealing of the deposited layers at lower temperatures, it was discovered that the missing rows of dimers are also arranged in $(2 \times n)$ structures with n increasing up to 12. Figure 4 presents an STM image which nominally corresponds to the (2×10) LEED pattern obtained after annealing at $T=270$ °C. This image graphically confirms that the missing rows of dimers are, in fact, ordered, but they still contain a significant number of irregularities, especially at the sites of row separation for $n=10$. It also shows that clusters of three-dimensional bismuth crystallites grow around the large vacancies. Such behavior is characteristic of Bi layers annealed at the lower temperatures.

The STM images of the $(2 \times n)$ structures display a significant dependence on the polarity of the voltage V_s applied between the sample investigated and the scanning tip. As a rule, an image obtained with $V_s > 0$, i.e., an image obtained in the empty-states mode, displays far more details in the atomic arrangement of the rows than an image obtained with $V_s < 0$. It should be noted that the observation of such a dependence during an STM experiment is not a trivial procedure, since the so-called "tip conditions," i.e., the tunneling conditions, vary with V_s , causing deterioration of the quality of the image and often resulting in its complete loss.²³

Figure 5 presents the STM images of the same portion of the surface with a (2×5) structure which were obtained in a specific "dual mode," i.e., with alternate application of a positive and a negative voltage V_s . The image obtained for $V_s > 0$ (Fig. 5a) shows the same periodicity as the image obtained when $V_s < 0$ (Fig. 5b), but reveals far more clearly the arrangement of the bismuth atoms in the (2×1) unit cells and the fact that the missing lines are missing rows of Bi atoms, as well as the fact that the lines present are actually rows of bismuth dimers, although they are inadequately resolved on this image. On the basis of the foregoing interpretation, we regard the linear structures separating the $(2 \times n)$ domains as missing rows of Bi dimers, which are usually observed on the STM images of $(2 \times n)$ structures in the filled-states mode (Fig. 5b). Besides the missing-Bi-dimer defects, as well as linear and rectangular vacancies, dislocation-type defects are also often discovered in the

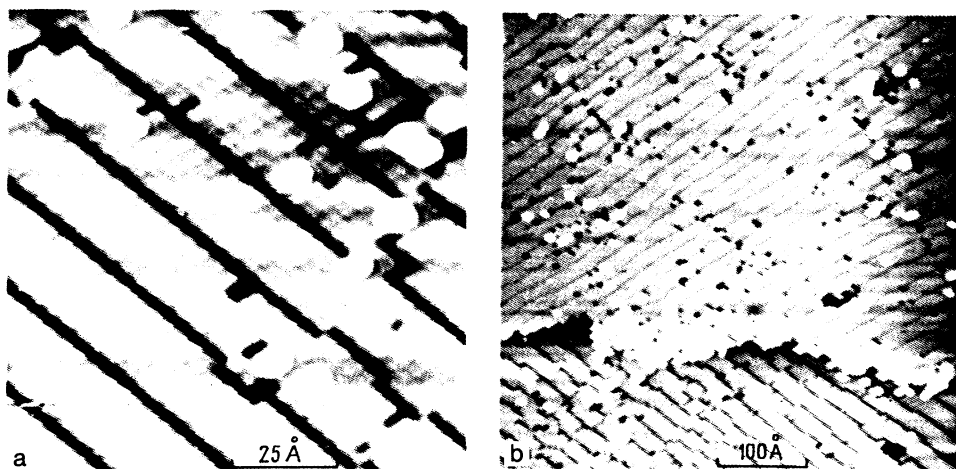


FIG. 3. a) STM image of a section of a Si(100)-(2 \times 1) surface after the deposition of Bi at room temperature followed by annealing at 378 °C (the voltage between the sample and the probe tip was $V_s = -1.6$ V, and the tunneling current was $I_t = 2.0 \times 10^{-11}$ A); b) STM image of a section of large area on the same surface.



FIG. 4. (2×10) structure obtained after annealing at $T=270$ °C with $V_s = -1.6$ V and $I_t = 2.0 \times 10^{-11}$ A.

striped domains of $(2 \times n)$ structures. Such defects are most noticeable on the STM images obtained in the unfilled-states mode, as is indicated by the arrow in Fig. 5a for the middle portion of three atomic stripes with a (2×5) structure. The magnified STM image of a portion of a similar surface (Fig. 6) clearly shows that they are the result of the displacement of a certain portion of the bismuth dimers by one atomic unit in the perpendicular direction. Such dislocation defects are often observed at positive values of V_s and can be regarded as a common defect in $(2 \times n)$ structures, which is characteristic of all similar systems. Figure 7 presents the structural model of the Bi/Si(100) system which we developed for this case. Since the dimensions of the Bi atoms (the atomic radius is 1.55 Å) significantly exceed the period of the Si lattice in the $\langle 110 \rangle$ direction (2.72 Å), a significant compressive elastic stress should be expected along the rows of bismuth dimers in this direction. This stress can be relieved by forming defects of the missing-row type with the resultant appearance of $(2 \times n)$ structures, where n depends on the annealing temperature. We call this mechanism “the formation of missing rows.” However, the elastic stress along the rows of dimers can also be relieved by simply displacing some of the rows

of dimers over a distance of one atom and creating a dislocation in the middle of a $(2 \times n)$ stripe. The formation of dislocation-type defects does not alter the configuration of the adsorption bonds of Bi in the sense that all the dangling bonds on the Si(100) surface can remain saturated as before. In such a model the Bi atoms are bonded to the surface by means of two dangling bonds of a Si dimer and are bonded to one another to form Bi dimers. Such a configuration does, in fact, result in the elimination of all the dangling bonds and is consistent with the inertness of the $(2 \times n)$ structure with respect to the adsorption of oxygen and, thus, with the passivation of such a surface.¹³

As we have already noted above, a $(2 \times n)$ phase with n less than 5 does not form, since we did not observe it on the STM images. Nevertheless, it was discovered that at higher annealing temperatures (and, therefore, smaller values of n) the missing rows of dimers in the (2×1) structures are more ordered, although the formation of a significantly larger number of defects of rectangular shape was observed in this case. In fact, the rows of Bi dimers which contain rectangular and linear defects can be regarded as local $(2 \times n)$ structures with n less than 5; however, sometimes these structures are not ordered and do not form large ordered striped domains. Therefore, we assume that as a consequence of the elastic stress appearing along the rows of dimers, the repulsive elastic interaction between neighboring missing rows of dimers for $n < 5$ can be so strong that the formation of linear or rectangular vacancies perpendicular to the missing rows will be energetically more favorable than the creation of missing rows separated by regular intervals smaller than $5a$. Therefore, the formation of $(2 \times n)$ structures with $n < 5$ turns out to be significantly more difficult, and the creation of vacancy-type defects begins.

As the annealing temperature increased further, these rectangular defects developed into larger spots of irregular shape, and, as a result, the surface investigated was found to consist of: a) islands with a (2×5) structure covered by Bi; b) sections of exposed Si(100). The STM images of such a surface with a partially desorbed Bi overlayer showed that the rows of Bi dimers are oriented perpendicularly to the rows of Si dimers. It is noteworthy, however, that the uncovered sections of the Si(100) surface displayed missing rows

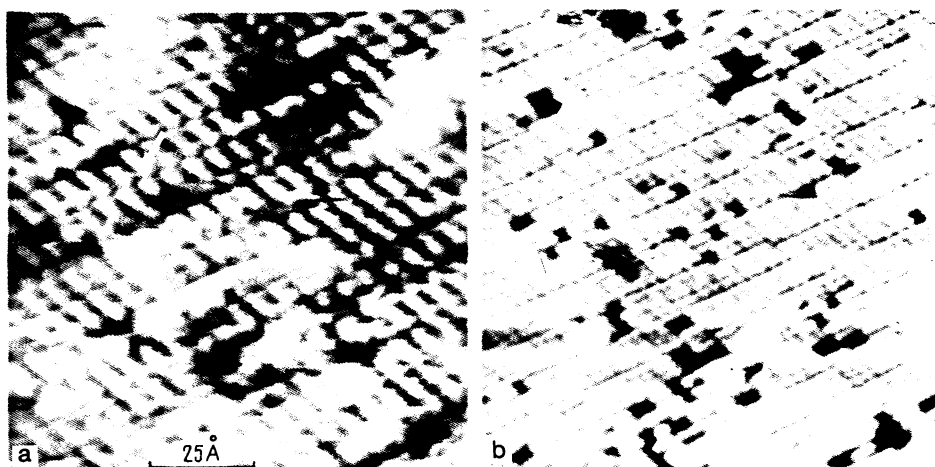


FIG. 5. STM images of a section of a surface with a (2×5) structure, which were obtained in the dual mode and display linear dislocations: a) $V_s = +1.2$ V; b) $V_s = -1.2$ V; c) $V_s = -1.2$ V, $I_t = 2.0 \times 10^{-11}$ A.

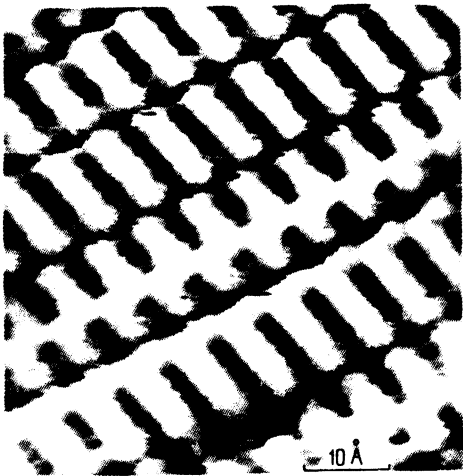


FIG. 6. Magnified STM image ($V_s = +1.2$ V, $I_t = 2.0 \times 10^{-11}$ A) of a section of a surface with a (2×6) structure, which clearly demonstrates the presence of dislocation-type defects.

of dimers with a $(2 \times m)$ structure, where m is close to 5, instead of the expected (2×1) structure.

As was noted above, however, after subsequent annealing at $T > 510$ °C, both the LEED patterns and the STM images displayed, a (2×8) structure, and only further annealing at $T = 540$ °C resulted in its complete disappearance and restoration of a clean (2×1) surface. We assume that since a large portion of the Bi must be desorbed at $T = 510$ °C, the observed (2×8) structure is, in fact, caused by the presence of a small quantity of Bi, which stabilizes the Si(100)- (2×8) structures like the Ni impurity which stabilizes the (2×8) structure on a Si(100) surface previously reported in Ref. 19.

As the STM images of the $(2 \times n)$ structures showed (Figs. 3–5), the rows of Bi adatoms are arranged perpendicularly to the rows of dimers on the Si(100) surface and generally have the same (2×1) periodicity. Clearly submitting that the Bi dimers are located in (2×1) unit cells and that the individual missing lines consist of linear chains of vacancies of Bi dimers, we can relate the distance na between the missing rows in a $(2 \times n)$ structure to the coverage θ of the surface with bismuth by the expression $\theta = 1 - a/na = 1 - 1/n$. In this context an individual observed $(2 \times n)$ structure can be regarded as an individual commensurate phase with the corresponding value of the coverage $\theta = 1 - 1/n$.

In principle, each $(2 \times n)$ structure with any integer n should form a commensurate phase; therefore, it is logical to expect that an infinite number of such phases should form as one monolayer (ML) is approached.²⁴ Therefore, as the Bi coverage increases from $\theta = 0.8$ ML to $\theta = 1.0$ ML, we can anticipate observing a sequence of commensurate phases with $(2 \times n)$ structures, among which the (2×5) structure will be dominant even in the presence of some thermal disordering caused by the restricted effect of the temperature. In this respect the coverage disparity above 1.0 ML is apparently the cause of both the appearance of specific $(2 \times n)$ structures and their dependence on $n = n(\theta)$.

The fact that the phase transitions occurring during annealing are irreversible even when three-dimensional bismuth crystallites coexist with a two-dimensional phase of this element convincingly demonstrates that the coverage disparity is not the main reason for such a transformation. Therefore, the significant elastic stress along the rows of dimers, which results from the great disparity between the dimensions of the Bi and Si lattices is responsible for the successive formation of $(2 \times n)$ structures. The energy of the elastic stress caused by distortion of the lattice along the bismuth rows is diminished by the formation of defects of the missing-row type during annealing. The elastic stress along the rows of Bi dimers is further weakened owing to the formation of dislocation-type defects and rectangular vacancies. The STM image of the ordered $(2 \times n)$ collections of missing rows (Fig. 3b) also graphically demonstrates the presence of a repulsive long-range interaction between neighboring missing Bi rows. Since the appearance of a considerable elastic stress was expected in an adsorbed layer of Bi, it was logical to expect the appearance of elastic repulsion between neighboring missing rows of Bi. In fact, Aruga and Murata showed that there is a rapid increase in the energy of the elastic repulsion between missing rows as the

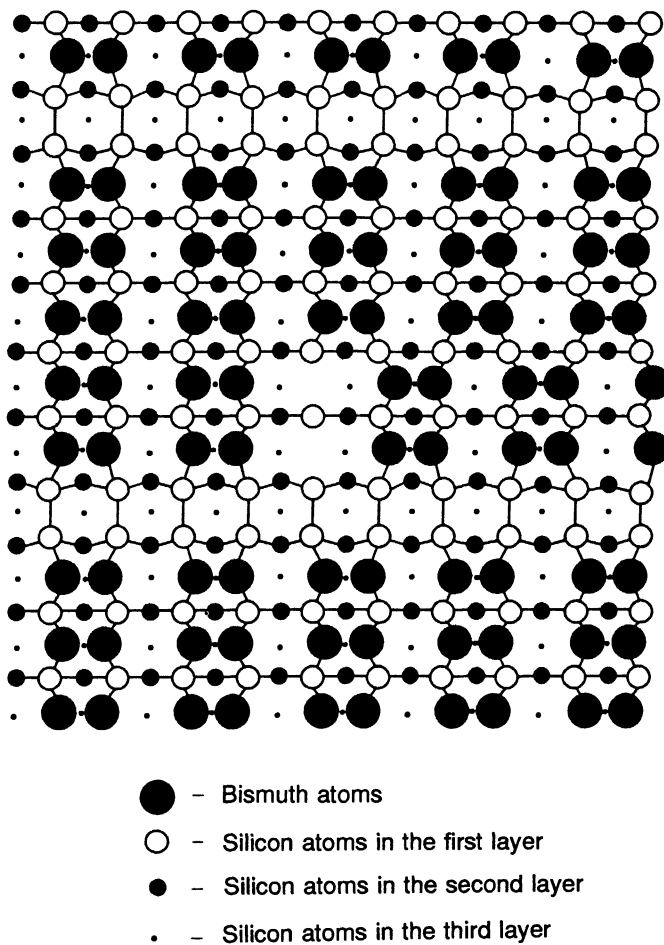


FIG. 7. Geometric model of the $(2 \times n)$ -Bi structure, showing Bi dimers, missing rows of Bi dimers, linear defects, and dislocation-type defects.

value of n in the $(2 \times n)$ reconstruction of the clean Si(100) surface decreases.¹⁷ This agrees well with the results presented above, which indicated that $(2 \times n)$ structures with $n < 5$ were not observed in the experiments and that the ordering was violated when defects of rectangular shape formed.

4. CONCLUSIONS

The atomic structure of the Si(100)- (2×1) -Bi surface has been investigated by STM and LEED. Series of well ordered $(2 \times n)$ superlattices with n varying from 5 to 12 have been discovered. A detailed analysis of the STM images has confirmed that the $(2 \times n)$ -Bi structure is the result of a periodic arrangement of missing rows of bismuth dimers within the (2×1) -Bi layer. It has been shown that the periodicity n in the $(2 \times n)$ structure depends on the coverage θ in accordance with the relation $\theta = 1 - 1/n$.

The fact that successive $(2 \times n)$ phases form as a function of θ and the annealing temperature attests to weakening of the elastic stresses in the rows of Bi dimers, which are subjected to compression, by creating missing rows and linear dislocations, as well as rectangular vacancies. The high degree of ordering of the $(2 \times n)$ phases suggests the presence of a strong long-range repulsive elastic interaction between the missing rows of Bi dimers.

However, it has been discovered for the phases with $n < 5$ that the ordering of the missing rows should be suppressed as a consequence of the strong repulsive interaction and the attendant formation of rectangular and linear defects.

We thank Prof. J. Nogami (University of Wisconsin–Milwaukee, U.S.A.) and Prof. Y. Hasegawa (University of Kyoto, Japan) for some useful discussions and valuable comments.

This research was performed with partial support from the International Science Foundation (Grant No. NYK000).

The main results of this work were reported to the Inter-

national Workshop–Seminar on Scanning Probe Microscopy, which was organized by the NATO Institute of Advanced Research (Germany, 1994).

- ¹B. N. J. Persson, Surf. Sci. Rep. **15**, 1 (1992).
- ²W. Monch, *Semiconductor Surfaces and Interfaces*, Springer-Verlag, New York–Berlin–Heidelberg, 1993.
- ³R. D. Mead and D. Vanderbilt, Phys. Rev. Lett. **63**, 1404 (1989).
- ⁴J. Tersoff, Phys. Rev. B **45**, 8833 (1992).
- ⁵R. Butz and S. Kaspers, Appl. Phys. Lett. **61**, 1307 (1992).
- ⁶F. K. Men, W. E. Packard, and M. B. Webb, Phys. Rev. Lett. **61**, 2469 (1988).
- ⁷R. M. Tromp, A. W. Denier van der Gon, and M. C. Reuter, Phys. Rev. Lett. **68**, 2313 (1992).
- ⁸R. Z. Bakhtizin, Ch. Park, T. Hashizume, and T. Sakurai, J. Vac. Sci. Technol. B **12**, 2052 (1994).
- ⁹R. I. G. Uhrberg, R. D. Bringans, R. Z. Bachrach, and J. E. Northrup, Phys. Rev. Lett. **56**, 520 (1986).
- ¹⁰R. S. Becher, T. Klitsner, and J. S. Vickers, J. Microsc. (Oxford) **152**, 157 (1988).
- ¹¹D. H. Rich, T. Miller, G. E. Franklin, and T.-C. Chiang, Phys. Rev. B **39**, 1438 (1989).
- ¹²S. Tang and A. J. Freeman, Phys. Rev. B **47**, 1460 (1993).
- ¹³T. Hanada and M. Kawai, Vacuum **41**, 650 (1990).
- ¹⁴T. Hanada and M. Kawai, Surf. Sci. **242**, 137 (1991).
- ¹⁵W. C. Fan, N. J. Wu, and A. Ignatiev, Phys. Rev. B **45**, 14 167 (1992).
- ¹⁶J. A. Martin, D. E. Savage, W. Moritz, and M. G. Lagally, Phys. Rev. Lett. **56**, 1936 (1986).
- ¹⁷T. Aruga and Y. Murata, Phys. Rev. B **34**, 5654 (1986).
- ¹⁸H. J. W. Zandvliet, H. B. Elswijk, and E. J. van Loenen, Phys. Rev. B **46**, 7581 (1992).
- ¹⁹H. Niehus, V. Kohler, M. Copel, and J. Demuth, J. Microsc. (Oxford) **152**, 735 (1988).
- ²⁰T. Sakurai, T. Hashizume, I. Kamiya, Y. Hasegawa, N. Sano, H. W. Pickering, and A. Sakai, Prog. Surf. Sci. **33**, 3 (1990).
- ²¹R. Z. Bakhtizin, C. H. Park, T. Hashizume, and T. Sakurai, Zh. Tekh. Fiz. **64**, 113 (1994) [Tech. Phys. **39**, 806 (1994)].
- ²²W. C. Fan, A. Ignatiev, and N. J. Wu, Surf. Sci. **235**, 1 (1990).
- ²³C. J. Chen, *Introduction to Scanning Tunneling Microscopy*, Oxford University Press, New York, Oxford, 1993, p. 1.
- ²⁴P. Bak, Rep. Prog. Phys. **45**, 587 (1982).

Translated by P. Shelnitz